

OTS adsorption: A dynamic QCM study

Yazan Hussain^a, Jacqueline Krim^b, Christine Grant^{a,*}

^a Department of Chemical and Biomolecular Engineering, Box 7905, North Carolina State University, Raleigh, NC 27695, USA

^b Department of Physics, Box 8202, North Carolina State University, Raleigh, NC 27695, USA

Received 14 July 2004; received in revised form 17 March 2005; accepted 31 March 2005

Available online 24 June 2005

Abstract

The uptake of octadecyltrichlorosilane (OTS) from an organic solution has been studied in situ and in real time by means of a quartz crystal microbalance (QCM) technique. Changes in both QCM frequency and resistance are reported for a range of OTS concentrations. In addition, the time dependence of OTS uptake has been used to calculate reaction constants. Silicon surfaces overall are characterized by higher levels of material uptake than gold.

© 2005 Elsevier B.V. All rights reserved.

Keywords: Quartz crystal microbalance (QCM); Octadecyltrichlorosilane (OTS); Adsorption

1. Introduction

Octadecyltrichlorosilane (OTS) can be readily deposited on hydroxylated silicon, which is of particular interest for the fabrication of microelectromechanical system (MEMS) devices. Surfaces coated with OTS exhibit high hydrophobicity and good chemical resistance. Proposed applications of OTS include its use as a self-patterned-mask for etching of SiO₂ on Si [1] and as a lubricant and anti-stiction material in MEMS devices [2,3].

Prior experimental characterizations of OTS films have been performed by several techniques including: atomic force microscopy [4,5], contact angle measurements [6], and high-resolution electron energy-loss spectroscopy (HREELS) [7]. A readily available but less widely used technique for surface studies in liquids is the quartz crystal microbalance (QCM). The QCM is highly sensitive to physical properties, particularly mass, of thin films deposited onto its surface electrode(s). It has been employed for a wide range of studies that include monitoring thin film deposition rates [8–10], polymer dissolution in supercritical CO₂ [11], chemical analysis [12], and hydration and swelling studies [13]. We employ it here to

monitor real-time OTS uptake in situ from a liquid environment.

The QCM operation depends on the sensitivity of its frequency to environmental variables including mass, viscosity of the surrounding medium, temperature, and pressure. The cumulative effect of all of these factors results in the total change in frequency.

For thin rigid films, the mass of the film is ideally related to the frequency change using the Sauerbrey equation:

$$\Delta F = - \left(\frac{2F_0^2}{\sqrt{\rho_q \mu_q}} \right) \Delta m \quad (1)$$

where F_0 is the resonance frequency of the unloaded crystal, ρ_q is the density of quartz ($= 2650 \text{ kg/m}^3$), and μ_q is the elastic shear modulus of quartz ($= 2.947 \times 10^{10} \text{ kg m}^{-1} \text{ s}^{-2}$). For changes in frequency that are less than 2% of F_0 , Sauerbrey's equation is considered highly accurate. Changes in frequency associated with viscous coupling can be a major component of the overall frequency response in liquid solutions. The viscous coupling may result from the viscoelasticity in the adsorbed material as well as from the surrounding liquid. When an oscillating crystal is in contact with a viscous medium, the shear wave in quartz will propagate through the medium causing high energy dissipation. This dissipation af-

* Corresponding author.

E-mail address: grant@ncsu.edu (C. Grant).

fects the frequency and the quality factor (Q), which can be quantified by measuring the change in the crystal resistance. In addition, changes in bulk and local viscosity can cause frequency changes. The relationship between medium viscosity (η) and resistance (R) was developed by Klavetter et al. [14]:

$$R = \frac{\pi}{8K^2 C_0} \left(\frac{\rho\eta}{\pi F_0 \mu_q \rho_q} \right)^{1/2} \quad (2)$$

where K^2 is the quartz electromechanical coupling coefficient ($= 7.74 \times 10^{-3}$), C_0 is the static capacitance of the crystal ($= 4.25$ pF), and ρ and η are the density and viscosity of the liquid. Similarly, the relation between the change in viscosity and ΔF is [15]:

$$\Delta F = - \left(\frac{F_0^3}{\pi \mu_q \rho_q} \right)^{1/2} (\rho\eta)^{1/2}. \quad (3)$$

A more complete analysis can be attained by measuring the acoustic impedance, which is usually performed by means of an impedance analyzer. Alternatively, it is possible to estimate the change in the crystal's impedance through analysis of frequency and resistance measurements. Lucklum and Hauptmann related the frequency shift, ΔF , and resistance shift, ΔR , to the acoustic load impedance using the following approximations [16]:

$$\frac{\Delta F}{F} = - \frac{\text{Im}(Z_L)}{\pi Z_{cq}} \quad (4)$$

$$\frac{\Delta R}{2\omega L} = \frac{\text{Re}(Z_L)}{\pi Z_{cq}} \quad (5)$$

where Z_L is the acoustic load impedance, Z_{cq} is the characteristic impedance of the quartz, ω ($= 2\pi F$) is the radial frequency, and L is the motional inductance of the unloaded crystal in the equivalent circuit. The authors calculated the impedance for different rubbery coatings in liquids with different viscosities. For example, a coating having a storage modulus (G') of 10^6 Pa, a loss modulus (G'') of 10^5 Pa, and a thickness of 100 nm immersed in 1 cP Newtonian liquid will have an impedance of ca. $8 + j6300$ Pa s m^{-1} . The acoustic load of the liquid alone is ca. $5600 + j5600$ Pa s m^{-1} . The value of L for the crystals used in this study was assumed to be 30 mH. Such analysis can be used to study the interfacial slippage of the adsorbed film [17]. Further details on the quartz crystal oscillator and its operation can be found elsewhere [18–20].

No prior studies of OTS uptake by means of QCM were found in literature. The most relevant work is that by Ruehe et al. [21] for the deposition of mono- and dichlorosilanes on Au surfaces. This paper presents a real-time study of OTS deposition from organic solvent onto both Si and metal coated QCM crystals. Both the frequency and resistance changes of the crystal in the liquid phase solution are evaluated. The overall objective is to provide information about the interactions and changes that occur on and close to the surface during uptake on materials of interest to MEMS applications.

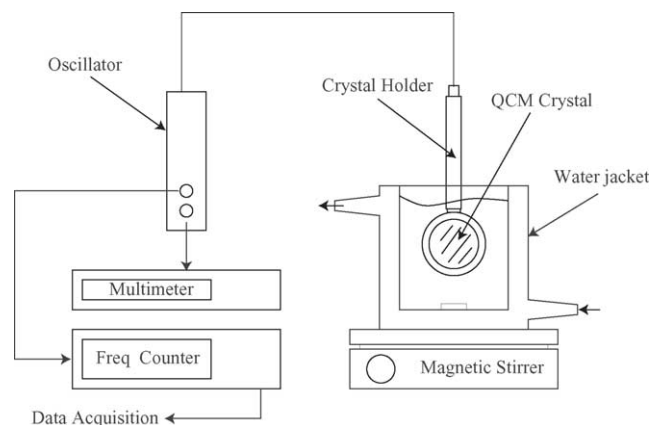


Fig. 1. Experimental setup.

2. Materials and method

2.1. QCM apparatus

Polished grade, 5 MHz, AT-cut QCM crystals obtained from Maxtek Inc. were used. A Teflon holder, also obtained from Maxtek, Inc., provided mechanical support and an electrical connection to drive the crystal. The holder allowed only one side of the crystal to be exposed to liquid. The crystals consisted of 2.5 cm diameter quartz disks upon which a thin layer of metal (either 1000 Å Si or 3400 Å Au) was vacuum deposited onto the liquid exposure side (1.3 cm diameter). A gold electrode (0.64 cm diameter), which was not exposed to the liquid, was deposited onto the reverse side of the crystal. A VC oscillator, obtained from Maxtek, was used to drive the crystal. The circuit provides two outputs: frequency and voltage. A frequency counter and a multimeter were used for frequency and resistance measurements. A schematic of the setup is shown in Fig. 1.

2.2. Experimental technique and materials

OTS (90%+), chloroform and hexadecane (99%+ anhydrous grade), dodecanethiol, and ethanol were obtained from Aldrich. The OTS was stored under vacuum. All materials were used as received without further purification.

Prior to each run, crystals were thoroughly washed with running water then rinsed with DI water, immersed in 0.05 M NaOH solution (~30 min), treated with UV/O₃ for 30 min, immersed in ethanol (~30 min), and, finally, treated again with UV/O₃. The second UV/O₃ treatment is to remove the remaining traces of contaminants and to generate the required hydroxylated surface [22]. This procedure was adopted with modification from previous work by Brzoska et al. [23].

After cleaning, crystals were immediately mounted in the holder and immersed in a solution of hexadecane and chloroform (4:1 by volume, as described in [2]). The solution was placed in a 250 ml Teflon beaker whose temperature was regulated to 20 ± 0.05 °C. Both frequency and voltage were

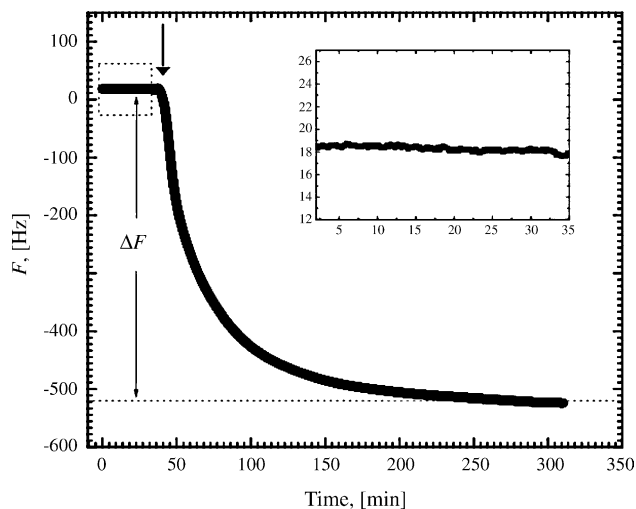


Fig. 2. Change in frequency for 5 MHz Si crystals upon injection of OTS (10 mM). The arrow indicates injection time. Insert is an enlargement of the region indicated by the box, to show the stability level.

recorded throughout the duration of the experiment. When the frequency signal reached a stable level (within 1–2 Hz as shown in the inset of Fig. 2), between 10 and 6000 μl of OTS was injected into 200 ml solution, yielding a concentration range up to 80 M. Frequency and voltage shifts were monitored throughout this process, and the run was ended when the frequency reached a new stable level. The difference between the two stable signals before and after injection was taken as ΔF .

3. Results and discussion

A representative plot of the QCM data for the adsorption of OTS on Si is shown in Fig. 2. The figure depicts three characteristic features of the data acquisition and analysis process. First, the frequency signal in the solution was stable to within 1–2 Hz for more than 30 min. Second, the frequency decreased almost immediately after OTS injection indicating fast adsorption on the surface. Finally, the frequency limits used to determine ΔF are noted on the figure.

Over the range of OTS concentrations studied, the values of ΔF ranged from 150 to 550 Hz. Using Eq. (1), this corresponds to a mass change of 1–5 μg , or 10–50 monolayers if a density of 20 \AA^2 per OTS molecule is assumed [24]. Although the OTS molecule with its inactive methyl endgroup is not expected to form multilayers, physical adsorption on the surface can occur [25,26]. Experimentally these excess deposits are usually removed by rinsing with fresh solvent before analyzing the sample [23]. Physical adsorption will have an effect on the frequency as well as the resistance through energy dissipation, as will be discussed later in this paper.

The high reactivity of OTS can affect the reproducibility of QCM results [21]. Our approach to this issue was as follows: first, the measurements were performed over a wide range

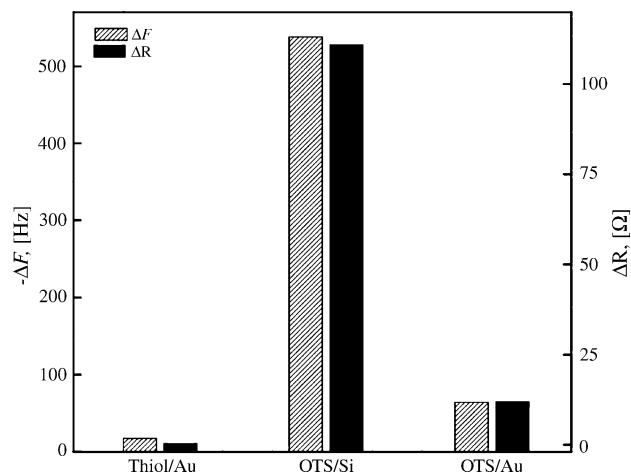


Fig. 3. Comparison of the change in frequency and resistance between: (1) dodecanethiol on Au from ethanol, (2) OTS on Si from $\text{C}_{16}\text{H}_{34}:\text{CHCl}_3$, and (3) OTS on Au from $\text{C}_{16}\text{H}_{34}:\text{CHCl}_3$. All runs were performed at 20 °C.

of concentrations to observe the general behavior. Second, repetition of a few randomly selected runs was done. Finally, the results from OTS are compared with other systems. The systems compared here were selected so that the reactivity of the molecule and the adsorbent–surface interaction were substantially different from the OTS/Si system. They include dodecanethiol ($\text{C}_{12}\text{H}_{25}\text{SH}$) uptake on Au from ethanol solution and OTS on Au with similar conditions to the OTS/Si. The results are shown in Fig. 3. For completeness, quantitative results are presented in this paper to compare different substrates and adsorbents in the same experimental system. Any attempt to compare absolute values of frequencies and ΔF values in another system must take into account differences in the experimental setup.

As can be seen from Fig. 3, using OTS on Si gave higher frequency and resistance changes than thiol and silane on Au surfaces. This is expected since the OTS is more reactive than the thiol. In the thiol-Au system, the interactions occur between the molecules and the surface, unlike OTS where the molecules are highly reactive to each other. Therefore, OTS is expected to cause larger changes in QCM response by forming a complex network on the surface which interacts with the molecules in the solution.

In contrast to the OTS/Si system, the adsorption of OTS on Au gave significantly lower frequency and resistance changes. This is also expected since the Au surface has less active sites (oxygen atoms) due to the inherent instability of the Au oxide layer, in contrast to that of Si (Note: Au–O bond strength is about 222 kJ mol^{-1} compared to 800 kJ mol^{-1} for Si–O [27]). From this observation it can be concluded that the changes in the solution properties are not the main factor affecting the QCM response.

The frequency change (ΔF) as a function of OTS concentration is shown in Fig. 4. It is interesting to note that at higher OTS concentrations ΔF tends to decrease instead of reaching a plateau. This may be due to the stronger interaction between OTS molecules at higher concentrations

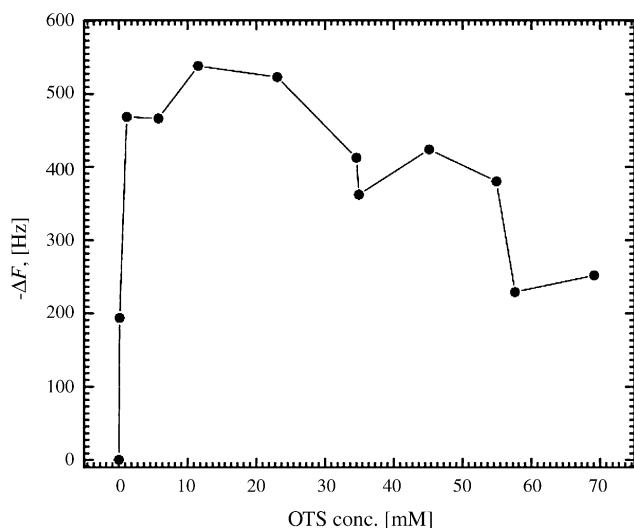


Fig. 4. Change in frequency for 5 MHz Si coated crystal upon deposition of OTS film from $C_{16}H_{34}\cdot CHCl_3$ (4:1 by volume) at different OTS concentrations.

which inhibits its free movement in the solution, causing less interaction with the crystal surface.

The above results suggest that the high affinity of Si surfaces to OTS molecules is inducing large changes in the vicinity of the surface. The nature of these changes and the extent that they interact with the surface are more difficult to address. However, calculating the acoustic impedance of the crystal can be used for this purpose by comparing the magnitudes of the real and imaginary parts of the impedance.

3.1. Acoustic impedance

The value of the complex acoustic impedance (Z_L) can provide insight into the nature of changes affecting the QCM. Lucklum and Hauptmann [13] theoretically calculated the impedance for a 5 MHz QCM crystal coated with 1 μm polymer films with different shear moduli. Their analysis suggests that a film in the glassy state will have low values for the real and imaginary parts of Z_L , whereas in the rubbery state the film will have a significant influence on both parts.

As shown in Fig. 5, both the imaginary and real parts have high values. According to the above discussion, this indicates a high viscous effect from the surrounding medium, which is translated into an increase in the viscosity of the region close to surface. This can be concluded by comparing the OTS/Si and OTS/Au systems. It is also evident from Fig. 5 that the imaginary part is slightly larger than the real part. This fact is expected since OTS does form a film on the Si surface.

3.2. Adsorption kinetics

The time-dependent frequency data can be used to study the adsorption kinetics. We will assume that the decrease in the resonance frequency represents the adsorption process, an approach that was used previously to study the kinet-

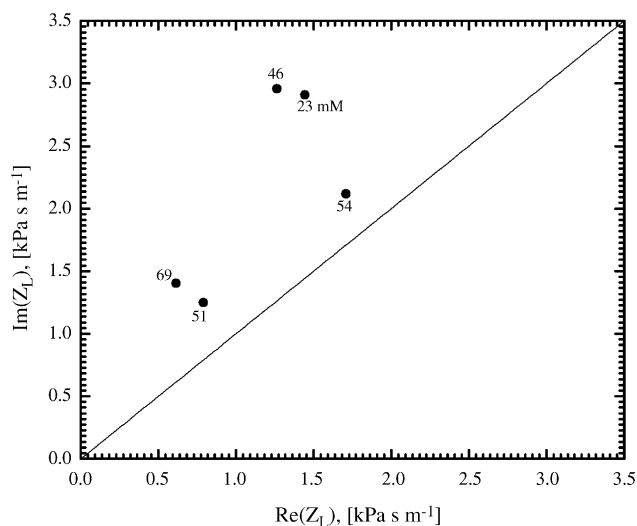


Fig. 5. Impedance diagram for the OTS coated crystals as calculated using Eqs. (4) and (5). OTS concentrations are indicated next to the points.

ics of alkanethiols adsorption [28,29]. Our evaluation begins with the premise that OTS adsorption follows a Langmuir mechanism. This mechanism involves a two step diffusion–adsorption process, where diffusion is assumed to be the limiting step in the case of OTS [6]. For such a mechanism, the reaction rate can be written as [6]:

$$\phi(t) = \frac{\beta}{\alpha} [1 - \exp(-\alpha t)] \quad (6)$$

where ϕ is the fraction of free active sites on the surface, $\alpha = C_b k_{af} + k_{ar}$ and $\beta = C_b k_{af}$. The parameters α and β can be obtained by fitting the frequency to Eq. (6). An example of QCM data with its theoretical Langmuir fit is shown in Fig. 6. From the relation between α and C_b , the values of k_{ar} and k_{af} were determined, see Fig. 7. The results of the reaction rate calculations, the equilibrium constant ($K_{eq} = k_{af}/k_{ar}$), and free energy of adsorption ($\Delta G = -RT \ln K_{eq}$) are shown in Table 1.

The large scatter in the data in Fig. 7 may be due to two factors. First, the frequency response may not be solely due to the OTS adsorption. It is also possible that the adsorption occurs in a short time interval of the frequency change, while the rest of the changes are due to viscous coupling effects. Second, the ideal assumption of Langmuir adsorption may need to be modified. As can be seen in Fig. 6, the frequency-time relation results in a relatively good fit to the experimental data. However, the behavior of ΔF with increasing concentration

Table 1
Kinetic and thermodynamic constants for OTS adsorption calculated from the QCM results assuming a Langmuir-type mechanism using Eq. (6)

Constant	Value
k_{af} (mM s ⁻¹)	0.14
k_{ar} (s ⁻¹)	0.001
K_{eq} (mM ⁻¹)	140
ΔG_{ads} (kcal/mol)	-7

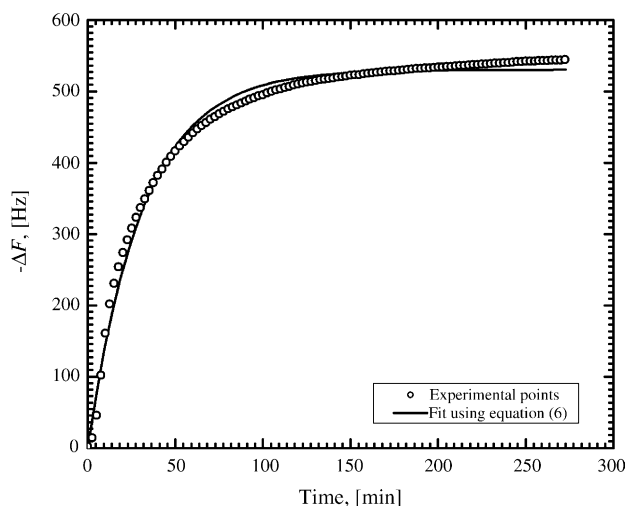


Fig. 6. Frequency response for 5 MHz Si QCM crystal after injection of OTS to a final concentration of 1 mM.

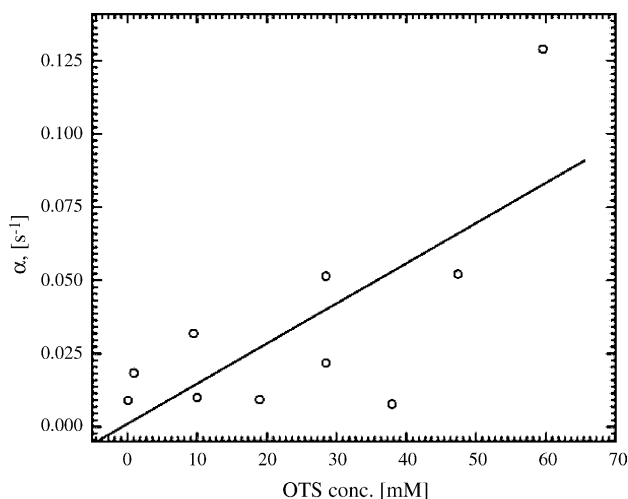


Fig. 7. Determination of rate constants for OTS absorption at 20 °C. The parameter $\alpha (= C_b k_{af} + k_{ar})$ was determined by fitting as discussed in the text.

(Fig. 4) does not follow this equation. Therefore, it may be necessary to modify the mechanism to take into account the effect of high OTS bulk concentrations.

4. Conclusion

The adsorption of OTS on Si surface was studied by measuring the change in QCM frequency and resistance, and the results were compared with thiol/Au and OTS/Au systems. The frequency shift associated with OTS adsorption on Si from hexadecane-chloroform solution was greater than 200 Hz. This shift is much larger than that observed with dodecanthiol. This may be explained by the presence of high viscous coupling near the surface, or the attachment of a slippery film of OTS to the surface. This was concluded from the decrease in the frequency shift at higher OTS concentrations.

The crystal resistance was coupled with frequency change to calculate the impedance of the deposits. The imaginary part of the impedance was comparable to the real part, a situation that can be compared to a rubbery polymer film. Finally, the reaction kinetics were determined by fitting the frequency-time data to Langmuir isotherm. The forward reaction rate constant is four orders of magnitude higher than the reverse constant.

Acknowledgements

This work was supported in part by Grant No. CMS-0087866 from the National Science Foundation and in part by a grant from the AFOSR No. F49620-01-1-0132 (JK).

References

- [1] T. Komeda, K. Namba, Y. Nishioka, Octadecyltrichlorosilane self-assembled-monolayer islands as a self-patterned-mask for HF etching of SiO₂ on Si, *J. Vacuum Sci. Technol. A: Vacuum Surf. Films* 16 (3) (1998) 1680–1685.
- [2] U. Srinivasan, M.R. Houston, R.T. Howe, R. Maboudian, Alkyltrichlorosilane-based self-assembled monolayer films for stiction reduction in silicon micromachines, *J. Microelectromech. Syst.* 7 (2) (1998) 252–260.
- [3] U. Srinivasan, R.T. Howe, R. Maboudian, Lubrication of polysilicon micromechanisms with alkylsiloxane self-assembled monolayers, in: B. Bhushan (Ed.), *Tribology Issues and Opportunities in MEMS*, Proceedings of the NSF/AFOSR/ASME Workshop held in Columbus, Ohio, 1998, pp. 597–606.
- [4] T. Balgar, R. Bautista, N. Hartmann, E. Hasselbrink, An AFM study of the growth kinetics of the self-assembled octadecylsiloxane monolayer on oxidized silicon, *Surf. Sci.* 523–535 (2003) 963–969.
- [5] C. Carraro, O.W. Yauw, M.M. Sung, R. Maboudian, Observation of three growth mechanisms in self-assembled monolayers, *J. Phys. Chem. B* 102 (1998) 4441–4445.
- [6] K. Efimenko, B. Novick, R.G. Carbonell, J.M. DeSimone, J. Genzer, Formation of self-assembled monolayers of semifluorinated and hydrocarbon chlorosilane precursors on silica surfaces from liquid carbon dioxide, *Langmuir* 18 (16) (2002) 6170–6179.
- [7] G.J. Kluth, M. Sander, M.M. Sunga, R. Maboudian, Study of the desorption mechanism of alkylsiloxane self-assembled monolayers through isotopic labeling and high resolution electron energy-loss spectroscopy experiments, *J. Vacuum Sci. Technol.* 16 (3) (1998) 932–936.
- [8] F. Caruso, T. Serizawa, D.N. Furlong, Y. Okahata, Quartz crystal microbalance and surface plasmon resonance study of surfactant adsorption onto gold and chromium oxide surfaces, *Langmuir* 11 (5) (1995) 1546–1552.
- [9] T.H. Ha, K. Kim, Adsorption of lipid vesicles on hydrophobic surface investigated by quartz crystal microbalance, *Langmuir* 17 (6) (2001) 1999–2007.
- [10] A. Weerawardena, C.J. Drummond, F. Caruso, M. McCormick, Real time monitoring of the detergency process by using a quartz crystal microbalance, *Langmuir* 14 (3) (1998) 575–577.
- [11] Y.-T. Wu, P.-J. Akoto-Ampaw, M. Elbaccouch, M.L. Hurrey, S.L. Wallen, C.S. Grant, Quartz crystal microbalance (QCM) in high-pressure carbon dioxide (CO₂): experimental aspects of QCM theory and CO₂ adsorption, *Langmuir* 20 (9) (2004) 3665–3673.
- [12] J. Wang, M.D. Ward, R.C. Ebersole, R.P. Foss, Piezoelectric pH sensors: AT-cut quartz resonators with amphoteric polymer films, *Anal. Chem.* 65 (19) (1993) 2553–2562.

- [13] M.T. Colberg, K. Carnes, A.E. Saez, C.S. Grant, K. Hutchinson, D. Hesterberg, Hydration of phospholipid films in aqueous environments, *Colloids Surf.* 153 (3) (1999) 483–495.
- [14] E.A. Klavetter, S.J. Martin, K.O. Wessendorf, Monitoring jet fuel thermal stability using a quartz crystal microbalance, *Energy Fuel* 7 (1993) 582–588.
- [15] S.J. Martin, V.E. Granstaff, G.C. Frye, Characterization of a quartz crystal microbalance with simultaneous mass and liquid loading, *Anal. Chem.* 63 (20) (1991) 2272–2281.
- [16] R. Lucklum, P. Hauptmann, The Δf - ΔR QCM technique: an approach to an advanced sensor signal interpretation, *Electrochim. Acta* 45 (2000) 3907–3916.
- [17] J. Ellis, G. Hayward, Interfacial slip on a transverse shear mode acoustic wave device, *J. Appl. Phys.* 94 (2003) 7856–7867.
- [18] V.E. Bottom, *Introduction of Quartz Crystal Unit Design*, Van Nostrand Reinhold electrical/computer science and engineering series, Van Nostrand Reinhold Company, 1982.
- [19] D.A. Buttry, M.D. Ward, Measurement of interfacial processes at electrode surfaces with the electrochemical quartz crystal microbalance, *Chem. Rev.* 92 (6) (1992) 1355–1379.
- [20] C. Lu, A.W. Czanderna, *Applications of piezoelectric quartz crystal microbalances, Methods and Phenomena: Their Applications in Science and Technology*, vol. 7, Elsevierff, 1984.
- [21] J. Ruehe, V.J. Novotny, K.K. Kanazawa, T. Clarke, G.B. Street, Structure and tribological properties of ultrathin alkylsilane films chemisorbed to solid surfaces, *Langmuir* 9 (1993) 2383–2388.
- [22] A. Ulman, *An Introduction to Ultrathin Organic Films: From Langmuir-Blodgett to Self-Assembly*, Academic Press, San Diego, 1991.
- [23] J.B. Brzoska, I.B. Azouz, F. Rondelez, Silanization of solid substrates: A step toward reproducibility, *Langmuir* 10 (11) (1994) 4367–4373.
- [24] F. Schreiber, Structure and growth of self-assembling monolayers, *Progress Surf. Sci.* 65 (5–6) (2000) 151–256.
- [25] L. Netzer, R. Iscovici, J. Sagiv, Adsorbed monolayers versus Langmuir-Blodgett monolayers—why and how? I. From monolayer to multilayer, by adsorption, *Thin Solid Films* 99 (1983) 235–241.
- [26] W.R. Ashurst, C. Yau, C. Carraro, C. Lee, G.J. Kluth, R.T. Howe, R. Maboudian, Alkene based monolayer films as anti-stiction coatings for polysilicon MEMS, *Sens. Actuators, A: Phys.* A91 (3) (2001) 239–248.
- [27] D.R. Lide (Ed.), *CRC Handbook of Chemistry and Physics* [electronic resource], third ed., Knovel, Norwich, NY, 2001.
- [28] D.S. Karpovich, G.J. Blanchard, Direct measurement of the adsorption kinetics of alkanethiolate self-assembled monolayers on a microcrystalline gold surface, *Langmuir* 10 (1994) 3315–3322.
- [29] H. Kima, S. Kwak, Y. Kim, B. Seo, E. Kim, H. Lee, Adsorption kinetics of alkanethiols studied by quartz crystal microbalance, *Thin Solid Films* 327–329 (1998) 191–194.